

Structural Morphological Optical and Photoluminescence Properties of ZrO₂ Nanoparticles Synthesized by Sol-Gel Method

N. Mahendran, S. Johnson Jeyakumar, M. Jothibas

PG&Research Department of Physics, TBML College, Porayar Tamil Nadu, India-609 307.

**Corresponding Author:*

E-mail[✉]: drsjohnson@rediffmail.com (Dr.S.JohnsonJeyakumar),

Abstract: Zirconia (ZrO₂) nanoparticles with monoclinic blended structure were successfully synthesized by sol-gel method using zirconium (IV) acetate hydroxide as the metal precursor, polyvinylpyrrolidone as the capping agent, and deionized water as solvent. The chemicals were mixed and stirred to form a homogeneous solution and hereafter directly underwent calcination to attain the pure nanocrystalline powder, which was confirmed by FTIR, UV, SEM, PL, and XRD analyses. The control over the size and optical properties of nanoparticles was achieved through the molarity change in calcination temperatures from 500°C. The obtained average particle sizes from XRD spectra images showed that the particle size increased with increasing calcination temperature. The optical properties which were investigated using a UV-Vis spectrophotometer showed a decrease in the band gap energy with increasing calcination temperature due to the enlargement of the particle size. These results prove that, by eliminating drying process (24 h) in the present thermal treatment method, size-controlled zirconia nanoparticles were conveniently manufactured with a reduction of synthesis time and energy consumption, suitable for large-scale fabrication.

Keywords; XRD, SEM, PL, UV, FTIR,

INTRODUCTION

ZrO₂ (zirconia) is a material of great technological importance, having good natural color, high strength, transformation toughness, high chemical stability, excellent corrosion resistance, and chemical and microbial resistance [1, 2]. ZrO₂ is a wide band gap p-type semiconductor that exhibits abundant oxygen vacancies on its surface. The high ion exchange capacity and redox activities make it useful in catalysis [3]. ZrO₂ is also an important dielectric material for potential application as an insulator in transistors in future nanoelectric devices [4]. ZrO₂ has three well-defined crystal phases, that is, cubic (c-ZrO₂), tetragonal (t-ZrO₂), and monoclinic (m-ZrO₂), under normal atmosphere and at different temperatures [5,6]. Generally, m-ZrO₂ phase is thermodynamically stable up to 1100°C, t-ZrO₂ phase exists in the temperature range of 1100–2370°C, and the cubic phase is found at high temperature above 2370°C [8,9,10]. Several techniques are available for producing zirconian nanoparticles, such as sol-gel method [11], vapor phase method [12], pyrolysis [13], spray pyrolysis [14], hydrolysis [15], hydrothermal [16], and microwave plasma [17]. However, these methods faced many limitation factors such as complicated procedures, high reaction temperature, long reaction time, toxic reagents and by-products use, and high cost of production, which made it difficult to prepare zirconian nanoparticles on a large-scale production. This process covers a variety of materials such as organic, inorganic hybrid and metallic materials. Nanostructured coatings developed by the sol gel technique provide enhanced functional or mechanical properties as well as purity, homogeneity and improved microstructure [18,19]. It does not require vacuum and allow fabricating a large area with low cost and at low processing temperature.

Recently, sol-gel method has been used in syntheses of several nanomaterials including metals ferrite nanoparticles, zinc oxide nanoparticles, cadmium oxide nanoparticles, and thermoluminescence nanomaterials. However, in the synthesis of ZrO_2 nanoparticles, a solution containing metal precursor and capping mediator is directly submitted to calcination, thus eliminating the drying process and reducing the preparation time and the energy consumption. Basically, ZrO_2 itself is an insulating direct wide gap metal oxide, with an optical band gap in the range 5.0-5.85 eV [20,21]. The earlier sol-gel methods for fabrication of metal oxide nanoparticles such as nanosized ZrO_2 powder, a necessity for large-scale industrial application. The technique is relatively environmentally friendly as no toxic material discharges into the drainage system. The effect of calcination temperature on the structural, particle size, and optical properties of ZrO_2 nanoparticles is also investigated using various techniques.

2. EXPERIMENTAL METHODS

2.1 Materials

$ZrOCl_2 \cdot 8H_2O$ and ammonia solution (91%) were purchased from Spectrum in India. All the above mentioned chemicals are of research grade that can be used without further purification.

2.2 Synthesis of ZrO_2 nanoparticles

The ZrO_2 nanostructures were synthesized by using a very simple and low cost method. $ZrOCl_2 \cdot 8H_2O$ was dissolved in distilled water in various vigorous stirring for 1 hr. Therefore ammonia solution was added into the solution drop wise while stirring until the pH value of the solution reached 10-14. While adding the ammonia. The finally white colored precipitate was containing. The $Zr(OH)_4$ precipitated was washed thoroughly with distilled water and centrifuged at 3000 rpm for 20 min to remove the residuals. The process was repeated several times until the precipitate was free from any trace impurities. The obtained $(ZrOH)_4$ precipitate was dried in an air hot oven at $100^\circ C$ for 1 hr and further calcined at $500^\circ C$ for 2 hrs resulting in the formation of (ZrO_2) nanoparticles.

2.3 Characterization of the samples

Structural analysis was carried out using X-ray diffractometry (XRD) spectrometer using CuK_α radiation ($\lambda = 1.5406 \text{ \AA}$) operated at 40 kV and 30 mA in the wide angle region of 2θ range from 30° to 70° . Morphology and microstructure were identified by scanning electron microscope (SEM Philip XL 30). Formation of ZrO_2 phase and available molecular bonds were investigated by the FTIR absorption spectrum. To investigate the optical properties of these nanoparticles, the absorbance spectra of the samples were obtained using UV-Vis-NIR spectrophotometer. The spectral absorption spectra were recorded using UV visible spectrometer (model: Lambda 35, make Perkin) in the wavelength range 300 to 1000 nm using quartz cuvettes at room temperature. The photoluminescence (PL) spectrum of the ZrO_2 nanoparticles dissolved in methanol has been measured using a spectrophotometer in the range of 400 to 4000 cm^{-1} (F-2500 FL Spectrophotometer, Hitachi). The electrical conductivity study is carried out by using Keithley 2636 B source meter.

3. RESULTANT DISCUSSION

3.1 Structural studies

The crystal structure in ZrO_2 nanoparticles sample with different molar concentrations is shown in Figure.1. The peak positions are in good agreement with the standard ZrO_2 (JCPDS:37-1475). The XRD spectra of powder sample were synthesized at 0.05M, 0.1M, 0.15M and 0.2M concentration.

The XRD spectra of sample powder optimized temperature 500°C have three resolved peaks at $2\theta=28.216, 31.5050, 35.3522$. which are indexed as reflection from (100), $\bar{1}11$, (002) and (311) planes respectively. These indexed peaks corresponding to pure monoclinic phase of the ZrO_2

The crystallite size has been inferred from 2θ and the full width at half maximum (FWHM) of ($\bar{1}11$) diffraction peaks on the basis of the Scherrer's relation

$$D = \frac{K\lambda}{\beta \cos \theta} \text{----- (1)}$$

Where D is the average crystallite size (Å), K is the shape factor (0.9), λ is the wavelength of X-ray (1.5406 Å) CuK α radiation, θ is the Bragg angle and β is the corrected the line broadening of the nanoparticles [22]. The calculated crystal size was found to increase with increase of molarity. It means that increase at higher molar concentration with decrease in FWHM of the peak. It is also evident from Table 1. for monoclinic [23] where d is the lattice spacing, a, b, c and β are the lattice parameters, d is interplanar spacing, (h, k, and l) are the miller indices, θ is the angle of corresponding peak and λ is the wavelength of X-ray used (1.5406 Å). The lattice constant showed a increase with increase of molarity

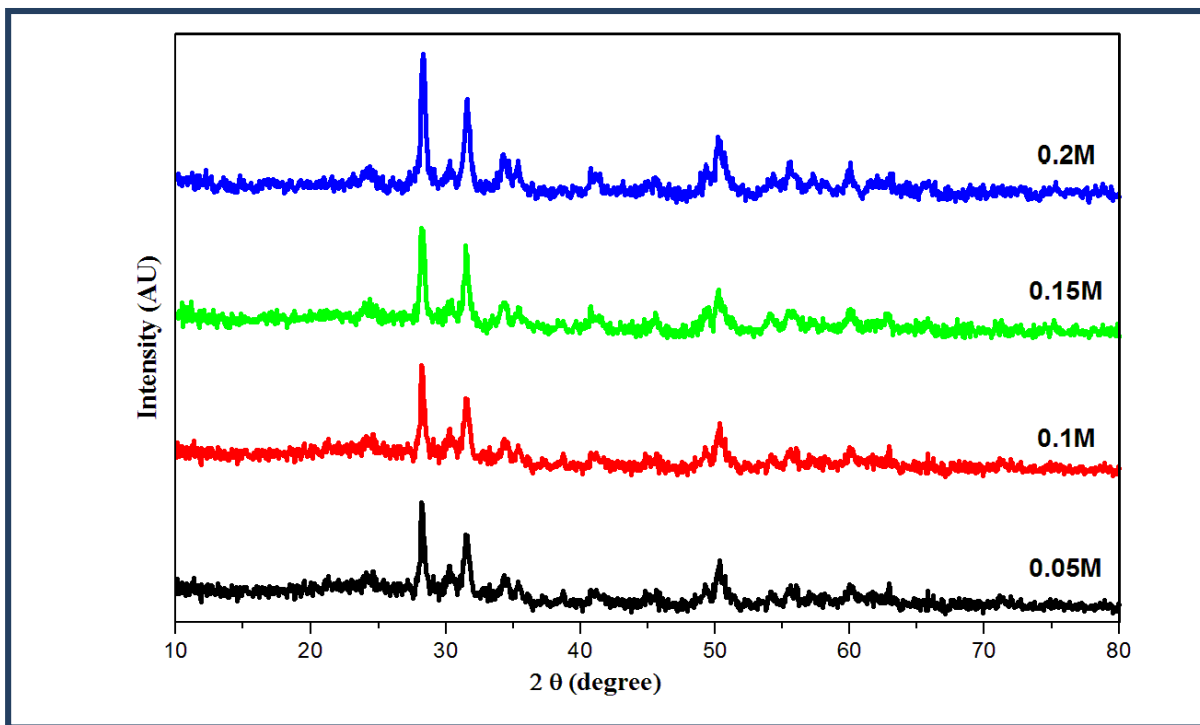


Figure.1 XRD Patterns of ZrO_2 nanoparticles for various molarity concentrations.

$$\frac{1}{d^2} = \frac{1}{\sin^2 \beta} \left[\frac{h^2}{a^2} + \frac{k^2 \sin 2\beta}{b^2} + \frac{l^2}{c^2} - \frac{2hlc \cos \beta}{ac} \right]$$

The structural parameters are calculated from the following equations [24],

Microstrain,
$$\epsilon = \frac{\beta \cos \theta}{4} \text{----- (3)}$$

Dislocation density,
$$\delta = \frac{1}{D^2} \text{----- (4)}$$

Table.1. Structural parameters of ZrO₂ nanoparticles

Molarity	2θ degree	Crystallite size(D) nm	Dislocation density δ x10 ¹⁴ lines/m ²	Microstrain ε	Lattice constants Å	Crystal structure
0.05M	28.2161	28.97	11.915	0.0012	5.312	Monoclinic
0.10M	28.2159	34.76	8.274	0.00104	5.31	Monoclinic
0.15M	28.2779	34.76	8.271	0.0010	5.312	Monoclinic
0.20M	28.2249	34.76	8.274	0.0006	5.31	Monoclinic

β= 99.218

The lattice defects like microstrain and dislocation density showed a decreasing trend with increasing molarity which may be due to the improvement of crystallinity as well as the high orientation along (111)direction (Figure.1).

3.2. Optical study

3.2.1. Evaluation of band gap energy

Optical characters of Zirconia (ZrO₂) nanoparticles were studied by UV absorption spectroscopy. The UV absorption spectrum of the nanoparticles as shown in Figure.2. The absorption edge was found at shorter wavelength in the UV region at 210 nm. The absorption co-efficient is calculated using the formula,

$$\alpha = \frac{2.303A}{l} \text{----- (5)}$$

where, A is the absorbance and l is the path length. The value of optical band gap is determined from the absorption spectra using the Tauc relation[25] ,

$$ah\nu = A(h\nu - E_g)^n$$

where, α is the absorption co-efficient, A is the constant having separate value for different transitions, hν is the photon energy and E_g is the band gap energy. The value of n depends upon the nature of transition. The values of n for allowed direct, allowed indirect, forbidden direct and forbidden indirect transitions are 1/2, 2, 3/2 and 3, respectively.

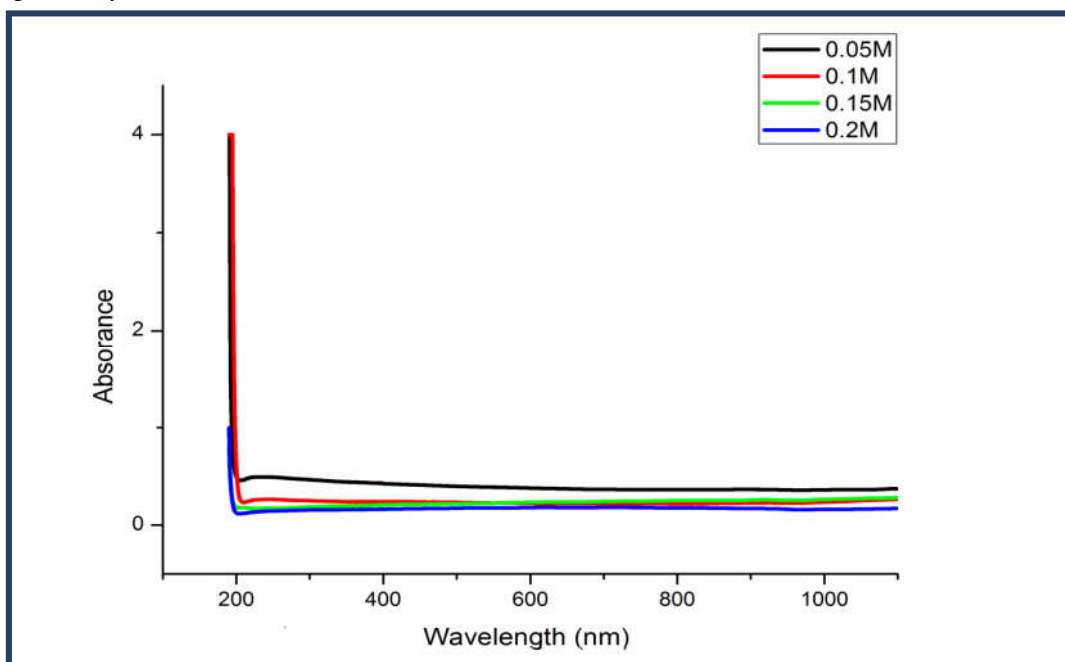


Figure. 2 Optical absorption spectra of ZrO₂ nanoparticles at various Molarities.

The band gap energies are found to be a negative number for $n = 2, 3/2$ and 3 , and hence the relationship fitting to the ZrO_2 is $n=1/2$, which confirms the allowed direct transition. Figure.3 shows the curves of $(\alpha h\nu)^2$ versus $h\nu$ for pure ZrO_2 nanoparticles prepared at different molarities. The E_g values are obtained by extrapolating the straight line portions of the graph to the X-axis. The measured energy band gaps from these plots are represented in Table 2. From this table, it can be observed that the E_g values varied from 4.8eV to 5.2eV for Pure ZrO_2 nanoparticles prepared at optimized temperature. The bandgap energy of semiconductors tends to decrease as the molarity is increased. An increased inters atomic spacing decreases the potential seen by the electrons in the material, which in turn reduces the size of the bandgap energy.

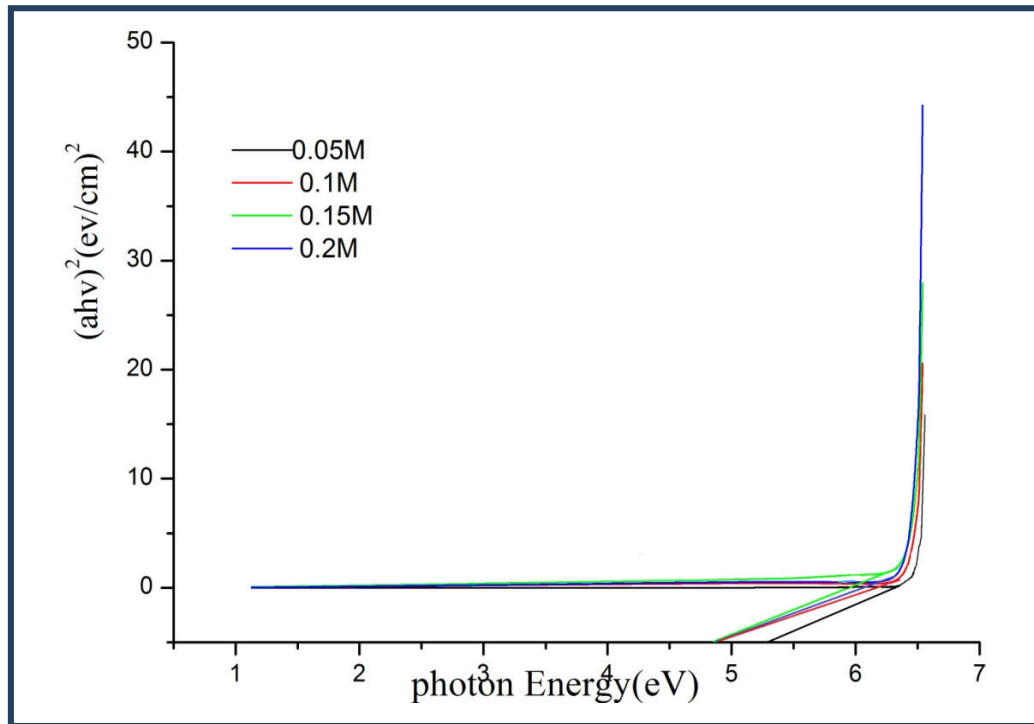


Figure. 3 The plot $(\alpha h\nu)^2$ versus $h\nu$ pure ZrO_2 nanoparticle

Table. 2 Variation of absorption edges and energy band gap of ZrO_2 nanoparticles at various molarity

Molarity M	Band gap energy(eV)
0.05	5.2
0.1	4.8
0.15	4.8
0.2	4.8

3.3 Functional group analysis of ZrO_2 nanoparticles

The FTIR spectra of synthesized sample at calcined at $500^\circ C$ in different molarity (0.05-0.2M) of ZrO_2 are as shown in Figure.4. The spectrum of ZrO_2 is related to the nature of materials, preparative procedures used, solid-state structure and so forth [26]. Looking at FT-IR spectra, it's clear that the ZrO_2 nanostructures still contain water molecules, since H_2O and CO_2 molecules have a property to be chemisorbed easily on the ZrO_2 surface, when they are exposed to the atmosphere [27]. The spectra were taken in the range $400-4000\text{ cm}^{-1}$. The main peaks at 470 cm^{-1} are due to the formation of Zr-O bonds and which are in the range of IR ($800-400\text{ cm}^{-1}$) photon modes of crystalline Zirconia [28].

The absorption band at 1552 cm^{-1} corresponds to the H-O-H bending vibration region is attributed to stretching of O-H group, characteristics of hydrated compound.

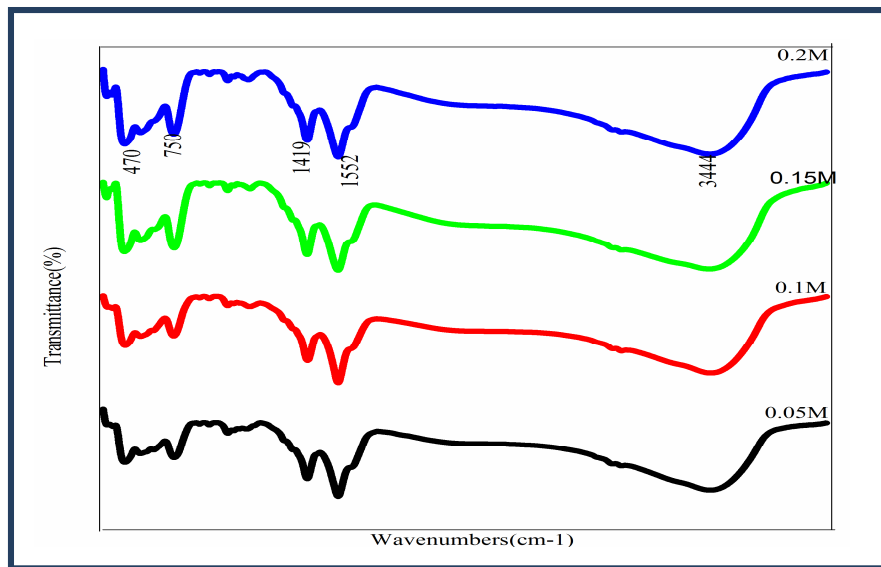


Figure. 4 FTIR spectra of ZrO_2 nanoparticles at various Molarities

3.4 Surface Morphological analysis

The Figure.5(a, b, c and d) the SEM micrographs of the surface of (ZrO_2)nanoparticles prepared at different molar concentrations. The surface morphology of the ZrO_2 nanoparticles is observed. But, it could not be viewed the grain size clearly. From the Figure5(a, b) one can find that, a microstructure consisted of many plateshaped crystalline particles. The microstructure formed is found to be uniform and compact which are interconnected by grains. These results suggested that, the size of the grains is large at low concentration; less than 0.1M. Further, it is reduced, when the molarity concentration is increased. There by the best uniform surface morphology is identified at 0.2M. However, the overall observation is that, the grain size is decreased and its surface becomes optically flat with increase the concentration. Pure ZrO_2 nanoparticles appears like plate in shape of size $\sim 1\mu\text{m}$. All these nanoparticles present in the size range of nm.

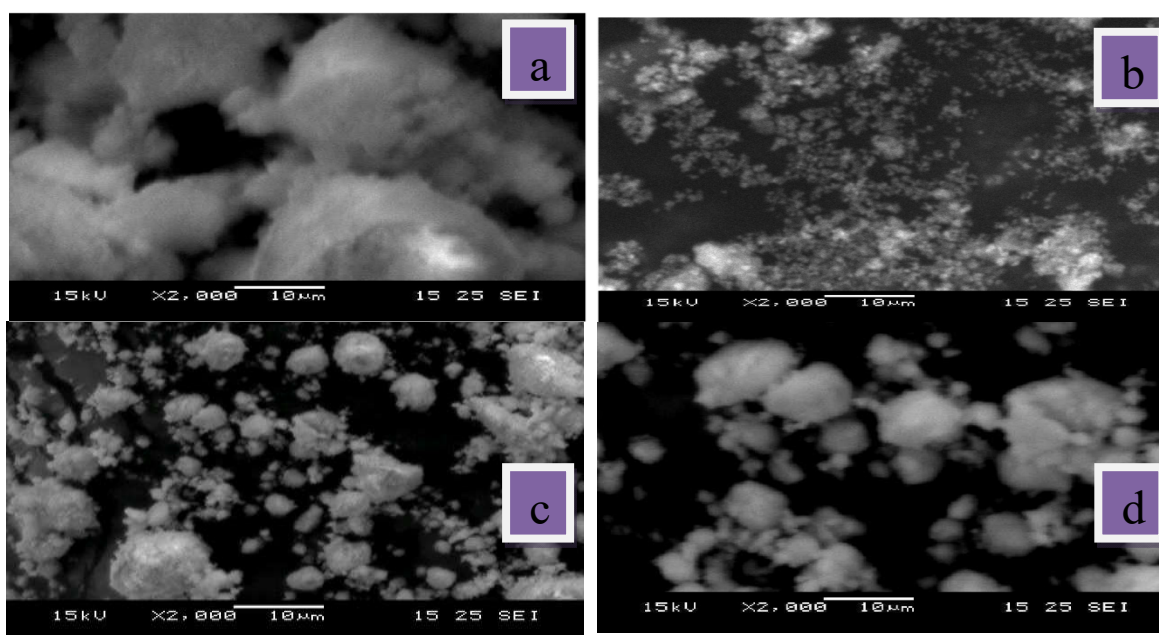


Figure.5(a-d) SEM images of ZrO_2 nanoparticles at different magnifications

3.5 Photoluminescence (PL)

The Photoluminescence (PL) spectra of zirconiananoparticles was recorded with a view to understand the formed nanoparticles on the emission properties of the materials. Photoluminescence emission curves of the molarity (0.05-0.2M) for zirconiananoparticles has a broad Visible emission band extending from 350 nm to 600 nm which nearly covers the entire visible range showing emission peaks for 0.15M and 0.2M at 359nm, 409nm, 443nm, 492 nm and 518 nm are obtained. The peaks at 359 nm excitation wavelength, 443nm and 492nm phosphors exhibit blue. The peaks are obtained in the Figure.6. All peaks range and shift including as shown in the Table.3

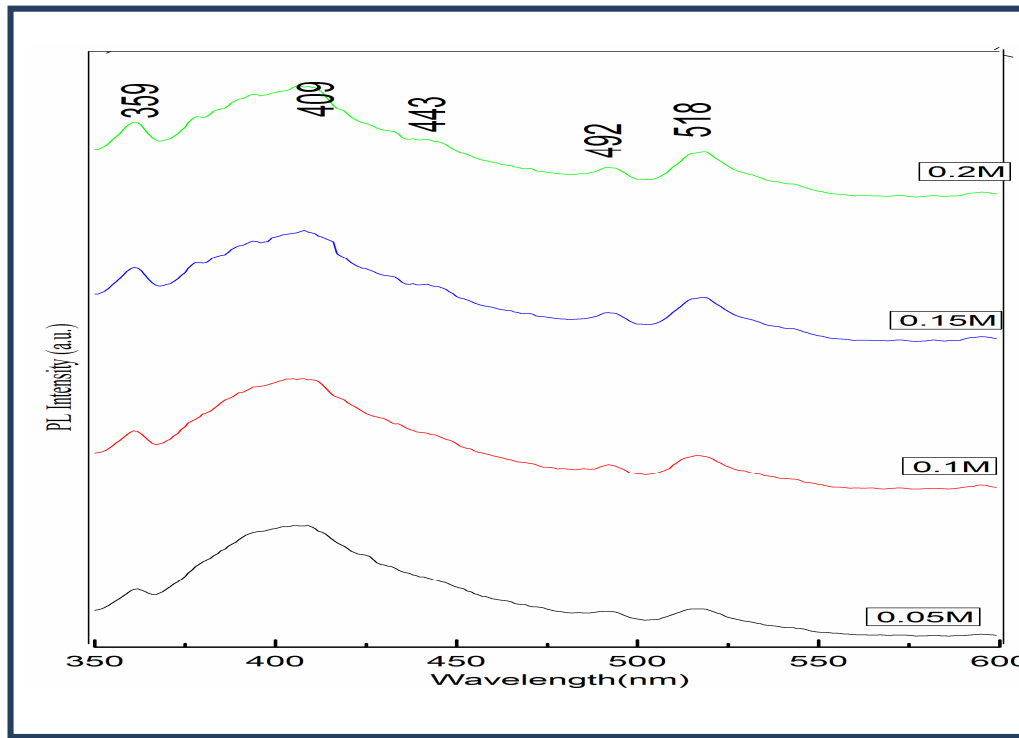


Figure. 6 The photoluminescence spectra of ZrO₂ nanoparticles at various Molarities.

Table. 3. The Photoluminescence spectra ZrO₂ nanoparticles.

Range(nm)	Colour
359-409	Green
443-492	Blue
500-596	Red /Orange

CONCLUSION

The ZrO₂ nanoparticles calcined at 500°C have been prepared by a sol-gel method. The study of XRD revealed that the synthesized ZrO₂ nanoparticle transformed monoclinic structure [JCPDS- NO-37 - 1475] ZrO₂ nanoparticles. The Optical properties were examined by the UV-Vis absorption spectrum. The band gap value was found to be 4.8eV to 5.2eV. The PL emission of the sample covers full nearly visible range attributed to the closed level emission which can be considered to be promoted by the morphology and size of the nanoparticles formed. Considering the growth and reproducibility of the ZrO₂ nanoparticles and visible emission found in the as formed sample provides better option for LED application.

REFERENCES

1. A. Hirvonen, R. Nowak, Y. Yamamoto, T. Sekino, and K. Niibara, *Fabrication, structure, mechanical and thermal properties of zirconia-based ceramic nanocomposites* *Journal of the European Ceramic Society*, 2006 26(8), 1497–1505.
2. J. C. Ray, D.W. Park, and W.S. Ahn, *Chemical synthesis of stabilized nanocrystalline zirconia powders*, *Journal of Industrial and Engineering Chemistry*, 2006, 12 (1),142–148.
3. J. L. Gole, S. M. Prokes, J. D. Stout, O. J. Glembocki, and R. Yang, *Unique properties of selectively formed zirconia nanostructures*, *Advanced Materials*, 2006, 18 (5),664–667.
4. G. Dutta, K. P. Hembram, G. M. Rao, and U. V. Waghmare, *Effects of O vacancies and C doping on dielectric properties of ZrO₂: a first-principles study*, *Applied Physics Letters*, 2006, 89 (20),202904.
5. S. Aysar, B. Keite, E. Saion, A. Zakaria, and N. Soltani, *Structural and Optical Properties of Zirconia Nanoparticles by Thermal Treatment Synthesis*, *Journal of Nanomaterials*, 2016,1-6.
6. H. Bensouyad, H. Sedrati, H. Debdoub, M. Brabimi, F. Abbas, H. Akkari, and R. Bensaha, *Structural, thermal and optical characterization of TiO₂:ZrO₂ thin films prepared by sol–gel method*, *Thin Solid Films*, 2010, 519 (1), 96–100.
7. R. Ashraf, S. Riaz, Z. N. Kayani, and S. Naseem, *Effect of Calcination on Properties of ZnO Nanoparticles*, *Materials Today: Proceedings*, 2015, 2 (10), 5468–5472.
8. L. Chen, T. Mashimo, E. Omurzak, H. Okudera, C. Iwamoto, and A. Yoshiasa, *Pure Tetragonal ZrO₂ Nanoparticles Synthesized by Pulsed Plasma in Liquid*, *The Journal of Physical Chemistry C*, 2011, 115 (19), 9370–9375.
9. Navio, Hidalgo, G. Colon, S. G. Botta, and M. I. Litter, *Preparation and Physicochemical Properties of ZrO₂ and Fe/ZrO₂ Prepared by a Sol–Gel Technique*, *Langmuir*, 2001, 17(1), 202–210.
10. A. Emeline, G. V. Kataeva, A. S. Litke, A. V. Rudakova, V. K. Ryabchuk, and N. Serpone, *Spectroscopic and Photoluminescence Studies of a Wide Band Gap Insulating Material: Powdered and Colloidal ZrO₂ Sols*, *Langmuir*, 1998, 14 (18), 5011–5022.
11. A. U. Limaye and J. J. Helble, *Effect of precursor and solvent on morphology of zirconia nanoparticles produced by combustion aerosol synthesis*, *Journal of the American Ceramic Society*, 2003, 86 (2), 273–278.
12. F. Heshmatpour and R. B. Aghakhanpour, *Synthesis and characterization of nanocrystalline zirconia powder by simple sol-gel method with glucose and fructose as organic additives*, *Powder Technology*, 2011, 205 (1-3),93–200.
13. H. Keskinen, P. Moravec, J. Smol, V. V. Levdansky, J. M. Makek, and J. Keskinen, *Preparation of ZrO₂ fine particles by CVD process: Thermal decomposition of zirconium tertbutoxide vapor*, *Journal of Materials Science*, 2004, 39 (15),4923–4929.
14. W. Nimmo, D. Hind, N. J. Ali, E. Hampartsoumian, and S. J. Milne, *The production of ultrafine zirconium oxide powders by spray pyrolysis*, *Journal of Materials Science*, 2002 37 (16),3381–3387.
15. S. Esposito, M. Turco, G. Bagnasco, C. Cammarano, and P. Pernice, *New insight into the preparation of copper/zirconia catalysts by sol–gel method*, *Applied Catalysis A: General*, 2011, 403 (1-2), 128–135.
16. S. Costacurta, P. Falcaro, S. Vezzù, M. Colasuonno, P. Scopece, E. Zanchetta, M. Guglielmi, and A. Patelli, *Fabrication of functional nanostructured coatings by a combined sol–gel and plasma-enhanced chemical vapour deposition method*, *Journal of Sol-Gel Science and Technology*, 2011, 60 (3), 340–3460.
17. A. Dittmar, D. L. Hoang, and A. Martin, *TPR and XPS characterization of chromia-lanthana-zirconia catalyst prepared by impregnation and microwave plasma enhanced chemical vapour deposition methods*, *Thermochimica Acta*, 2008, 470 (1-2),40–46.
18. S. Riaz, M. Bashir, S. S. Hussain, and S. Naseem, *Effect of Mn-doping Concentration on the Structural and Magnetic Properties of Sol-Gel Deposited ZnO Diluted Magnetic Semiconductor*, *Proceedings of the 2013 International Conference on Advanced Computer Science and Electronics Information*, 2013.
19. J.A. Navio, M.C. Hidalgo, G. Colon, S. G. Botta, and M. I. Litter *Preparation and Physicochemical Properties of ZrO₂ and Fe/ZrO₂ Prepared by a Sol-Gel Technique* *Langmuir* 2001, 17, 202-210.
20. D. S. S. Padovini, D. S. L. Pontes, C. J. Dalmaschio, F. M. Pontes, and E. Longo, *Facile synthesis and characterization of ZrO₂ nanoparticles prepared by the AOP/hydrothermal route*, *RSC Adv.*, 2014, 4 (73), 38484.

21. A. R. Puigdollers, F. Illas, and G. Pacchioni, *Structure and Properties of Zirconia Nanoparticles from Density Functional Theory Calculations*, *The Journal of Physical Chemistry C*, 2016, 120 (8), 4392–4402.
22. M. Jothibas, S. Johnson Jeyakumar, C. Manoharan, I. KartharinalPunithavathy, P. Praveen, and J. Prince Richard, *Structural and optical properties of zinc sulphide nanoparticles synthesized via solid state reaction method*, *Journal of Materials Science: Materials in Electronics*, 2016, 28 (2), 1889–1894.
23. A. Sumner, *Doubtful value Eukaryotic Chromosomes (1991)*. Edited by R. C. Sobti and G. Obe. Narosa Publishing House, New Delhi/Springer-Verlag, Berlin. 295pp. DM 178, *BioEssays*, 1992, 14 (2), 141–142.
24. J. Prince Richard, I. KartharinalPunithavathy, S. Johnson Jeyakumar, M. Jothibas, and P. Praveen, *Effect of morphology in the photocatalytic degradation of methyl violet dye using ZnO nanorods*, *Journal of Materials Science: Materials in Electronics*, 2016, 28 (5), 4025–4034.
25. S. Kumar, S. Bhunia, and A. K. Ojha, *Effect of calcination temperature on phase transformation, structural and optical properties of sol-gel derived ZrO₂ nanostructures*, *Physica E: Low-dimensional Systems and Nanostructures*, 2015, 66, 74–80.
26. A. K. Singh and U. T. Nakate, *TiO₂ Microwave Synthesis, Electrophoretic Deposition of Thin Film, and Photocatalytic Properties for Methylene Blue and Methyl Red Dyes*, *ISRN Nanotechnology*, 2014, 1–8.
27. S. Kumar, S. Bhunia, and A. K. Ojha, *Effect of calcination temperature on phase transformation, structural and optical properties of sol-gel derived ZrO₂ nanostructures*, *Physica E: Low-dimensional Systems and Nanostructures*, 2015, 66, 74–80.
28. L. A. Perez-Maqueda and E. Matijevic, *Preparation and characterization of nanosized zirconium (hydrated) oxide particles*, *Journal of Materials Research*, 1997, 12 (12), 3286–3292.
29. H. Zhang, X. Fu, S. Niu, and Q. Xin, *Blue emission of ZrO₂:Tm nanocrystals with different crystal structure under UV excitation*, *Journal of Non-Crystalline Solids*, 2008, 354 (14), 1559–1563.